The effects of occlusion on single miniplate osteosyntheses of the mandible

Thomas R. Katona
Department of Orthodontics and Oral Facial Genetics, Indiana University School of Dentistry
Department of Mechanical Engineering, Purdue University School of Engineering and Technology
IUPUI, Indianapolis, Indiana

Indiana University
School of Dentistry
1121 W. Michigan St.
Indianapolis, IN 46202

Telephone: (317) 274-3383
FAX: (317) 278-1438
Email: tkatona@iu.edu

Running title: Occlusion and single miniplate osteosyntheses

Key words: occlusion, forces, miniplate, osteosynthesis, static equilibrium, fracture, mandible

ABSTRACT

Aim: Miniplate osteosyntheses of a fractured mandible is a complex structural engineering problem that has been modeled experimentally, analytically and numerically. In general, the more realistic the model, the more difficult it is to appreciate its nuances. Thus, a purpose of this paper is to present a basic analytical model that illustrates the most fundamental principles of static equilibrium as it applies to the mechanics of single miniplate osteosynthesis designs. The second purpose is to use the model to demonstrate the effects of changes in occlusion on the loads experienced by the structures.

Materials and methods: The 3 equations of static equilibrium were derived from the free-body-diagram of the distal segment of a vertically fractured reduced mandible. The equations were solved parametrically with variations in plate screw locations, anterior-posterior locations of occlusal contact, and occlusal contact force direction, including the simulation of sticky foods.

Results: The results indicate a profound effect of occlusal contact force location and direction on the magnitudes and/or directions of the forces acting on the screw and the miniplate, and on the location and magnitude of the interfragmental bone-bone compression force.

Conclusions: In some respects, this model is as barebones as is possible. Atypically however, it includes occlusal contact force direction. The results strongly suggest that all analyses of plating systems should account not only for occlusal contact force location and magnitude, but also its direction.

The effects of occlusion on single miniplate osteosyntheses of the mandible

INTRODUCTION

Mandibular miniplate osteosynthesis is a challenging structural engineering problem because of anatomical intricacies, diverse materials and loading variability. Finite Element Analysis (FEA)(Arbag et al., 2008; Bohluli et al., 2010; Kavanagh et al., 2008; Rangan et al., 2013; Sarkarat et al., 2012; Sato et al., 2012; Takahashi et al., 2010; Vajgel et al., 2013) is the most powerful and adaptable tool for the design and analysis of these structures. But all such numerical (as well as experimental, analytical, clinical and animal) models engender shortcomings stemming from simplifying assumptions. Furthermore, the understanding and interpretation of FEA results often require a technical background that is generally beyond that of non-engineers. And, none of the typical analyses lend themselves to the formation of intuitive or commonsensical comprehension of the critically relevant engineering principles.(Katona, 2011)

Thus, a relatively simple, but rigorous, analytical model is presented as a better suited approach for the demonstration of the fundamental mechanics of plating system design. Furthermore, the model is used to explore the loading effects of often ignored aspects of occlusion.

MATERIALS AND METHODS

Figure 1a is the free-body-diagram (FBD) of a fractured/plated distal mandibular segment showing all external forces, relevant dimensions and the x-y coordinate system. **T** is the occlusal contact force. **P** is the force applied to the screw by the plate, hence, to the bone segment. (By convention, bolding designates a vector quantity, whereas plain text refers to its magnitude.) The directions of the **T** and **P** force vectors are defined by θ_T and θ_P, respectively, measured counter-clockwise from the positive x-direction, **Figs 1a** and **b**. As examples, flat-plane occlusion is designated by $\theta_T = 270° = -90°$, while $\theta_T = 90°$ simulates sticky foods. **B**, the interfragmental bone-bone contact force across the fracture, is only allowed to be compressive (assuming no healing), hence, $\theta_B = 0°$.

For the problem to be tractable with basic statics analysis, the model must be in a statically determinate configuration, meaning that there can be only 3 unknowns; all else must be specified. The designated unknowns are the horizontal (P_x) and vertical (P_y) components of **P** and the magnitude of **B** (B). (P_x and P_y can be readily converted into equivalent expressions in terms of P and θ_P, and vice versa.) The 3 equations of static equilibrium, based on the FBD (**Fig 1a**) are:

$$\sum F_x = 0: \; P_x + B + T_x = 0 \qquad (1)$$

$$\sum F_y = 0: \; P_y + T_y = 0 \text{ and} \qquad (2)$$

$$\sum M_P = 0: \; -T_x(d - c) + T_y a + B(c - e) = 0 \qquad (3)$$

So from (3),

$$B = [T_x(d - c) - T_y a]/[c - e].$$

Then, from (1), $P_x = -B - T_x = -([T_x(d - c) - T_y a]/[c - e]) - T_x$, or

$P_x = [T_x(e - d) + T_y a]/[c - e]$ and from (2),

$P_y = -T_y$.

Thus, the 3 unknowns (P_x, P_y and B) are calculated. Also, $P = (P_x^2 + P_y^2)^{½}$ and $\theta_P = \tan^{-1}[P_y/P_x]$. And as **T** is defined by its magnitude (T = 1.0 N in all calculations) and direction (θ_T), $T_x = T\cos\theta_T = \cos\theta_T$ and $T_y = T\sin\theta_T = \sin\theta_T$.

As mentioned above, it is prescribed that the bone-bone contact force (**B**) across the fracture interface is in the horizontal direction (*i.e.*, frictionless bone-bone contact) and that, for geometric reasons, it can act either at the inferior border of the mandible (e = 0 mm, $\mathbf{B_1}$) or at its superior border (e = 30 mm, $\mathbf{B_2}$). The equations of static equilibrium (Equations 1 – 3) were solved with both possibilities, but only the solution in which **B** acted to the right ($\theta_B = 0°$) was accepted because a leftward acting **B** ($\theta_B = 180°$) would indicate tension across the fracture, which, of course, is impossible without healing. (As a consequence of the principle of force transmissibility,(Beer et al., 2013) the horizontal distance between the plate screw and the fracture line is irrelevant.)

Another invoked basic concept of mechanics is the treatment of the plate as a 2-force body, meaning that no moments of couples act on it, and therefore, the forces that act on its ends must align with the plate. Thus, the plate must be in either pure tension or pure compression. Essentially, the long slender plate is being modelled as a truss element, (Beer et al., 2013) a common practice in structural analysis.(Beer et al., 2013) The direction of **P** (θ_P) can be used to ascertain if the plate is in compression (if **P** has an anterior component, $\theta_P = 0° \pm 90°$) or tension (if **P** has a posterior component, $\theta_P = 180° \pm 90°$), **Figs 1b** and **c**.

d (40 mm), e (0 mm or 30 mm) and T (1.0 N, the magnitude of the occlusal contact force, **T**) were kept constant in all calculations, while c (28, 20 or 10 mm), a (38, 5 or -3 mm) and θ_T (-180 to 0.0° in +0.2° increments) were parametrically varied. And as noted above, all calculations for the 3 unknowns (P_x, P_y and B, or equivalently, P, θ_P and B) were performed with **B** acting at e = 0 and e = 30 mm, but only solution sets with compression across the fracture ($\theta_B = 0°$) were kept. Note that this is a linear model so, for example, T = 20 N (vs. the defined 1 N) would require that the calculated force magnitudes (P and B) be multiplied by a factor of 20.

RESULTS

The results of the static equilibrium calculations for the 3 unknowns (P, θ_P and B) are presented in graphical form (**Figs 2a** – **10a**) and as corresponding force vector representations (**Figs 2b** – **10b**). **Figures 2**, **3** and **4** are for the plate screw at (c =) 28 mm above the inferior border of the mandible or 2 mm from its superior height. The screw is lower (c = 20 mm) in **Figs 5**, **6** and **7**, and even lower (c = 10 mm) in **Figs 8**, **9** and **10**. Results for anterior tooth contact (a = 38 mm) are shown in **Figs 2**, **5** and **8**, posterior contact that is anterior to the screw (a = 5 mm) in **Figs 3**, **6** and **9**, and for contact located posterior to the screw (but anterior to the fracture, a = -3 mm) in **Figs 4**, **7** and **10**. (The 3 screw and 3 occlusal contact locations are diagrammed in **Fig 1a**.) Results for sticky foods are presented in **Fig 11**.

DISCUSSION

Caution must be exercised in generalizing the presented outcomes. The results should be examined from an engineering viewpoint and then from the clinical perspective. The underlying

physics is governed by the Newton's Laws – based principles of static equilibrium. With the occlusal contact location defined, the plate screw position specified on the fractured segment, and as the occlusal contact force sweeps through its range of prescribed directions, there must be a specific relationship between the magnitude of **P** (the force applied to the screw by the plate), direction of **P** (θ_P, hence the orientation of the plate, and tension vs. compression in the plate), magnitude of **B** (the interfragmental bone-bone contact force) and its location (inferior or superior border of the mandible). This unique relationship between the unknowns is rigorously delineated by the 3 equations of static equilibrium that were derived above.

Using **Fig 6** (a = 5 mm and c = 20 mm) as the exemplar, in the range of θ_T = -180 – -104.1° (-104.1° is the vertical dashed line), it is required that θ_P = 180.0° to 76.1°. This means that the force exerted by the plate on the screw (**P**) must be directed directly posteriorly (θ_P = 180.0°) when θ_T = -180.0° and it must be directly upward (θ_P = 90.0°) by the time θ_T = -116.6°, circle (○) on left. To the left of that circle, the plate is in tension because $\theta_P > 90.0°$. But in the interval between θ_T = -116.6° to -97.1° (*i.e.*, between the 2 circles), **P** has an anterior component ($\theta_P < 90.0°$), so within that interval, the plate is in compression. To the right of θ_T = -97.1° (circle on the right), the plate is once again in tension because $\theta_P > 90.0°$.

Between θ_T = -180.0° and -104.1°, the magnitude of **B** decreases from 2.0 N (which is twice that of the occlusal force) to 0.0 N, at which time, the bone-bone contact shifts from the superior edge of the fracture to its inferior border, and its magnitude, along with that of **P** starts to increase. Note that the shift in the bone-bone contact location takes place whenever the line-of-action (LOA) of **T** crosses the dashed line (**Fig 6b**) that connects the occlusal contact point with the screw. This θ_T transition angle (in this instance, -104.1°) is given by: $\theta_T = \tan^{-1}[(d - c)/a] - 180°$. (When the LOA of **T** is above the plate screw, **T** produces a counter-clockwise moment on the fractured segment, hence the bone-bone contact force (**B**) must be at the upper end of the fracture. The opposite occurs when the LOA passes below the plate screw.) The straight dashed lines in **Figs 2b** – **10b** illustrate the various θ_T transition angles.

Anatomic constraints render many of the equilibrium configurations impossible. For instance, for equilibrium requiring θ_P = 135° (plate in tension) or θ_P = 315° (plate in compression), **Figs 1b** and **c**, and depending on the relative location of the screw, the plate's distal end would have to be impossibly located on a molar crown, or beyond, for the plate to span the fracture. As a specific example, in **Fig 6b**, for θ_T = -90° (flat plane occlusion), the plate would reach the superior crest of the bone short of bridging the fracture. In this figure, only the --50° and the -160° configurations span the fracture.

Cusp anatomy imposes additional limitations. Forty degree cusps allow $\theta_T = -90 \pm 40°$, or a range of $-130° < \theta_T < -50°$, indicated by the shaded regions in **Figs 2a** – **10a**. Even so, forces on the screw (P) and/or the healing bone (B) can reach ~3 N (**Figs. 5a** and **9a**) and 4.5 to 6 N (**Figs 4a** and **8a**). These represent a 3 to 6-fold larger forces on the screw and bone than on the occluding teeth. With sticky foods, **Fig 11**, 20x force magnifications can be reached. Thus, even a mildly adhesive food substance has the potential to generate huge forces on the screw, plate and bone.

Most, perhaps all, experimental and FEA miniplate studies have been limited to a single occlusal contact force direction, typically flat-plane occlusion.(Arbag et al., 2008; Bohluli et al., 2010; Rangan et al., 2013; Ribeiro-Junior et al., 2010; Sarkarat et al., 2012; Sato et al., 2012; Shetty et al., 1995; Takahashi et al., 2010; Vajgel et al., 2013) Restricted to flat-plane occlusion, this study would produce only the θ_T = -90° results. Hence, in each of the **Figs 2a** – **10a**, only the 3 data points indicated by □ in **Fig 6a** would be present. And in **Figs 2b** – **10b**, only the "-

90" labelled **T**, **P** and **B** force vectors could be shown. This would represent a massive loss of information about the loads experienced by the screw, plate and bone.

Furthermore, a recent study demonstrates that individual occlusion/disclusion cycles are characterized by complex sets of multidirectional transient occlusal forces.(Katona and Eckert, 2017) Thus, in the analysis of miniplate related load bearing structures, it is imperative that a range of occlusal force directions be considered because that is realistic and because, as demonstrated herein, occlusal contact force directions are critical determinants of structural loads.

Insofar as occlusion is concerned, only the effects of occlusal contact force (**T**) location (a) and its direction (*i.e.*, cusp angulation, θ_T) have been considered. The magnitude of **T** was held constant at 1.0 N, but as previously noted, the calculated magnitudes of **P** and **B** are linearly proportional to the magnitude of **T**. Other aspects of occlusion (vertical dimension of occlusion and occlusal plane height, for example) that affect **T**, independent of muscle forces,(Katona, 1989) were not considered.

In broad terms, the clinical implication of the statically determinate equilibrium relationships is that the specific combination of screw location (c) and plate orientation (θ_P) that is required to maintain equilibrium for a particular **T** (as defined by its a and θ_T), cannot maintain equilibrium with a **T** that has a different a and/or θ_T. Yet, single miniplate reconstructions are frequently used successfully. There are explanations for this inconsistency.

Under some circumstances, meshing of the rough fractured bone surfaces can provide a measure of stability that, due to the frictionless bone-bone contact assumption, is absent in this model. The rough bone-bone surface interaction can generate a shear force component along the fracture line. However, its magnitude is unknown and impossible to realistically estimate, so it would have to be included as an additional (the fourth) unknown variable. Another added unknown quantity, a bending moment in the plate, would be present if more than one screw anchored the plate on one, or both, sides of the fracture. But as explained above, treating the miniplate as a truss element is acceptable engineering practice with such a slender member – the moment component is relatively inconsequential. Nonetheless, in some instances, these 2 loads (bone-bone generated shear force along the fracture line and bending moment in the plate) combine to produce an adequately strong structure. Thus, this model does not explain the successful applications of single miniplate osteosyntheses, but more importantly, it does shed light on their failures.

In any case, the 3 available equilibrium equations are sufficient to solve for 3 unknowns. P, θ_P and B were chosen for this project. Including more than 3 unknowns (adding, for example, the bone-bone shear force along the fracture or the bending moment within the plate) would render this model into a statically indeterminate configuration, meaning that the 3 equilibrium equations would be inadequate. Such problems can be approached with greatly more complicated strength-of-materials calculations that involve the stresses and strains within the structures. But the overwhelmingly preferable approach to such complex problems is the numerical FEA, some of which are listed in the Introduction. But that approach defeats a purpose of this project, namely the application of a "no frills" tractable analytical method. This approach facilitates the visualization and the intuitive understanding of the force/geometry relationships.

Despite its simplicity, this model highlights some engineering concerns that can be generalized to miniplate mandibular osteosyntheses of all kinds: (1) Not only are occlusal contact force magnitude and location critical determinants of the mechanical environment, so is

its (frequently ignored) direction. (2) Besides tension, there is also the potential for compression (hence buckling) within the plate. (3) Because tension between fractured bone segments is impossible, to maintain equilibrium, the interfragmental bone-bone contact location must shift. (4) The magnitudes of the forces on the plate, screws and the bone-bone contact can be substantially larger than the occlusal force. The most significant conclusion is that occlusal contact force direction should always be taken into account (point 1), otherwise points 2 – 4 may not be evident.

REFERENCES

Arbag, H., Korkmaz, H.H., Ozturk, K., Uyar, Y., 2008. Comparative evaluation of different miniplates for internal fixation of mandible fractures using finite element analysis. J Oral Maxillofac Surg 66, 1225-1232. 10.1016/j.joms.2005.11.092

Beer, F.P., Johnston, E.R., Mazurek, D.F., 2013. Vector Mechanics for Engineers - Statics, 10th ed. McGraw-Hill, NY.

Bohluli, B., Motamedi, M.H., Bohluli, P., Sarkarat, F., Moharamnejad, N., Tabrizi, M.H., 2010. Biomechanical stress distribution on fixation screws used in bilateral sagittal split ramus osteotomy: assessment of 9 methods via finite element method. J Oral Maxillofac Surg 68, 2765-2769. 10.1016/j.joms.2010.03.014

Katona, T.R., 1989. The effects of cusp and jaw morphology on the forces on teeth and the temporomandibular joint. J Oral Rehabil 16, 211-219.

Katona, T.R., 2011. A qualitative engineering analysis of occlusion effects on mandibular fracture repair mechanics. J Dent Biomech 2011, 752741. 10.4061/2011/752741

Katona, T.R., Eckert, G.J., 2017. The mechanics of dental occlusion and disclusion. Clin Biomech (Bristol, Avon) 50, 84-91. 10.1016/j.clinbiomech.2017.10.009

Kavanagh, E.P., Frawley, C., Kearns, G., Wallis, F., McGloughlin, T., Jarvis, J., 2008. Use of finite element analysis in presurgical planning: treatment of mandibular fractures. Ir J Med Sci 177, 325-331. 10.1007/s11845-008-0218-z

Rangan, V., Raghuveer, H.P., Rayapati, D.K., Shobha, E.S., Prashanth, N.T., Sharma, R., 2013. The influence of stress distribution in four different fixation systems used in treatment of mandibular angle fractures – a three-dimensional finite element analysis. Oral Surgery 6, 186-192. 10.1111/ors.12037

Ribeiro-Junior, P.D., Magro-Filho, O., Shastri, K.A., Papageorge, M.B., 2010. In vitro evaluation of conventional and locking miniplate/screw systems for the treatment of mandibular angle fractures. Int J Oral Maxillofac Surg 39, 1109-1114. 10.1016/j.ijom.2010.06.019

Sarkarat, F., Motamedi, M.H., Bohluli, B., Moharamnejad, N., Ansari, S., Shahabi-Sirjani, H., 2012. Analysis of stress distribution on fixation of bilateral sagittal split ramus osteotomy with resorbable plates and screws using the finite-element method. J Oral Maxillofac Surg 70, 1434-1438. 10.1016/j.joms.2011.05.017

Sato, F.R., Asprino, L., Consani, S., Noritomi, P.Y., de Moraes, M., 2012. A comparative evaluation of the hybrid technique for fixation of the sagittal split ramus osteotomy in mandibular advancement by mechanical, photoelastic, and finite element analysis. Oral Surg Oral Med Oral Pathol Oral Radiol 114, S60-68. 10.1016/j.tripleo.2011.08.027

Shetty, V., McBrearty, D., Fourney, M., Caputo, A.A., 1995. Fracture line stability as a function of the internal fixation system: an in vitro comparison using a mandibular angle fracture model. J Oral Maxillofac Surg 53, 791-801.

Takahashi, H., Moriyama, S., Furuta, H., Matsunaga, H., Sakamoto, Y., Kikuta, T., 2010. Three lateral osteotomy designs for bilateral sagittal split osteotomy: biomechanical evaluation with three-dimensional finite element analysis. Head Face Med 6, 4. 10.1186/1746-160X-6-4

Vajgel, A., Camargo, I.B., Willmersdorf, R.B., de Melo, T.M., Laureano Filho, J.R., Vasconcellos, R.J., 2013. Comparative finite element analysis of the biomechanical stability of 2.0 fixation plates in atrophic mandibular fractures. J Oral Maxillofac Surg 71, 335-342. 10.1016/j.joms.2012.09.019

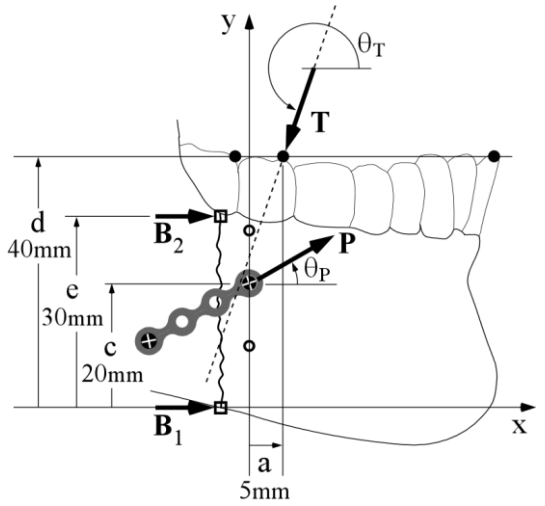

Fig. 1a

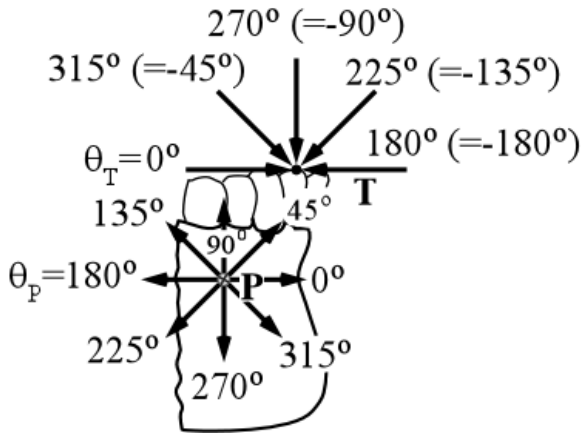

Fig. 1b

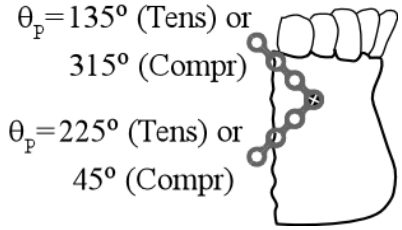

Fig. 1c

Figure 1. (a) Free-body-diagram (FBD) of the distal bone segment (drawn to-scale) of a vertically fractured/plated mandible. (**P** is the force *acting on the screw* (bone) with its line-of-action (LOA) defined by the plate orientation. This depicts compression in the plate.) The locations of occlusal contact points (3 solid circles, from the anterior to the posterior, at a = 38, 5 and -3 mm), plate screws (3 open circles, from the inferior to the superior at c = 10, 20 and 28 mm) and bone-bone contact (2 squares at e = 0 and 30 mm) are used in the calculations. The dashed line is the LOA of **T**. (b) Examples of θ_T and θ_P, with (c) the associated plate tension vs. compression.

Figures 2 - 10. (a) Calculated results (P, B and θ_P) as functions of θ_T for the 9 combinations (hence the 9 figures) of 3 screw height locations (c = 28, 20 and 10 mm) and 3 occlusal contact locations (a = 38, 5 and -3 mm). The shaded areas indicate the geometric limits on θ_T imposed by cusps up to 40°. (b) Some of the results in (a) shown graphically, to scale, as force vector arrow representations. The horizontal and vertical axes are in mm, so the three landmarks (occlusal contact point, screw, bone-bone contact) are shown by the small open circles. All force vector arrow magnitudes are drawn to a scale of 10 mm = 1 N, thus the prescribed 1 N magnitude of **T** is always the length of 2 squares. All labels refer to the prescribed value of θ_T. As an example, the "-90" labeled P, B and θ_P are all associated with θ_T = -90° (flat-plane occlusion). **B** is drawn either at e = 0 mm (inferior border of the mandible) or e = 30 mm (superior height of the fracture), whichever corresponds to bone-bone compression. (In Figs 4b and 8b some **P** lengths are drawn as P = 3.2 N to maintain uniform graph scales – the actual magnitudes are in parentheses.)

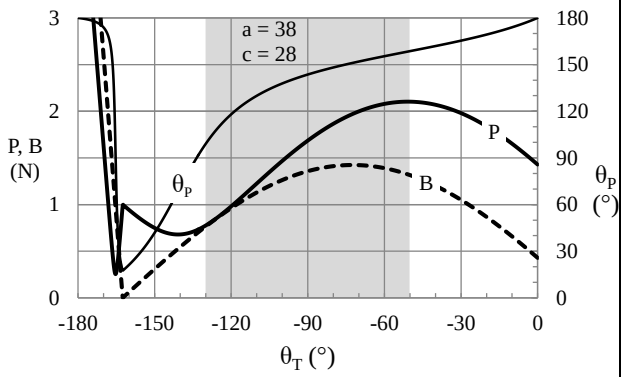

Fig. 2a

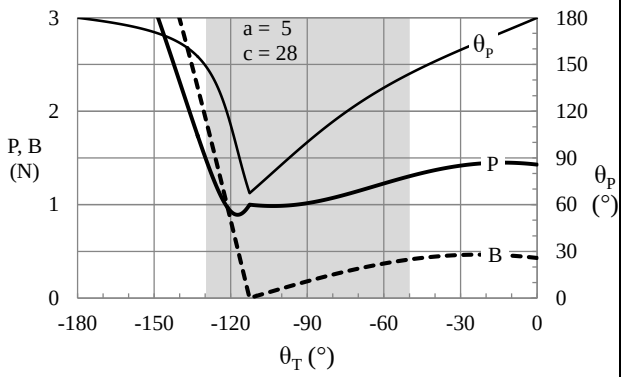

Fig. 3a

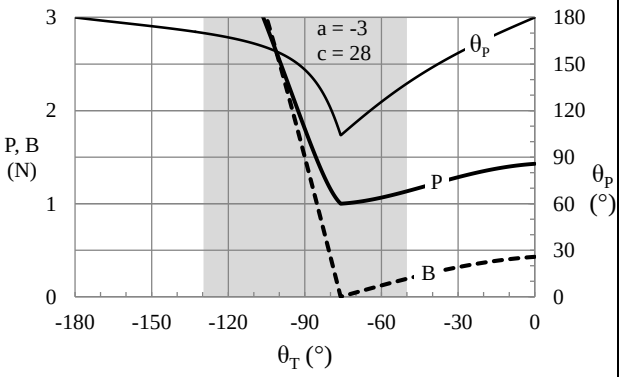

Fig. 4a

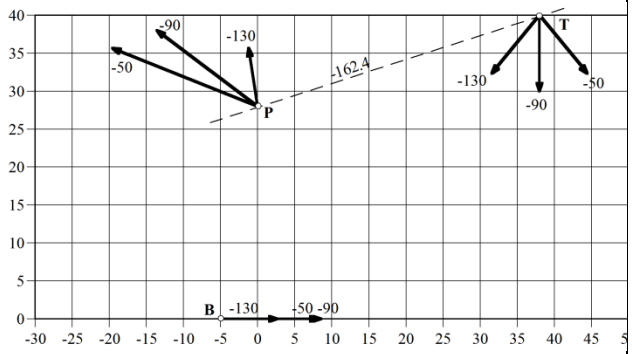

Fig. 2b *c* = 28 mm, *a* = 38 mm.

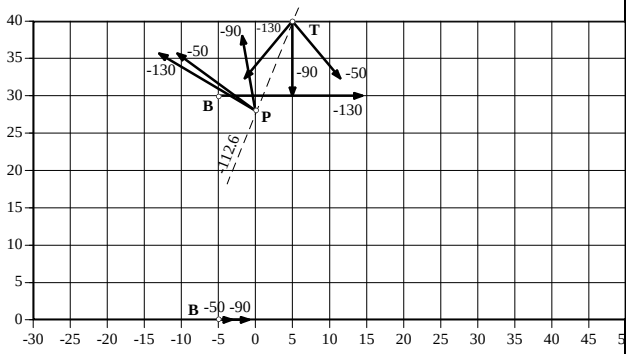

Fig. 3b *c* = 28 mm, *a* = 5 mm.

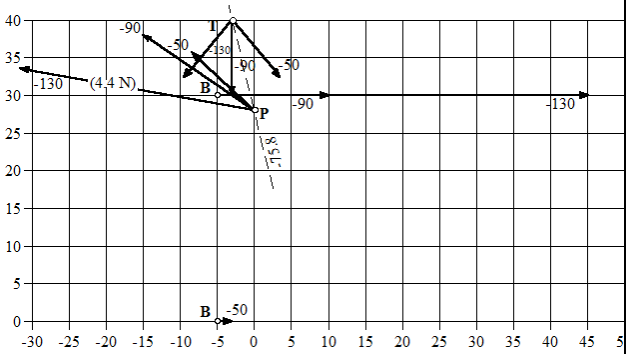

Fig. 4b *c* = 28 mm, *a* = -3 mm.

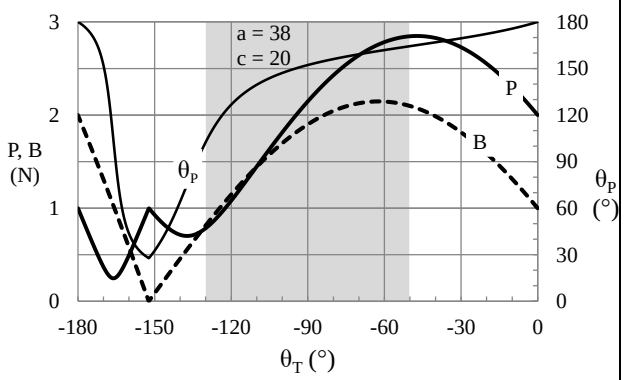

Fig. 5a

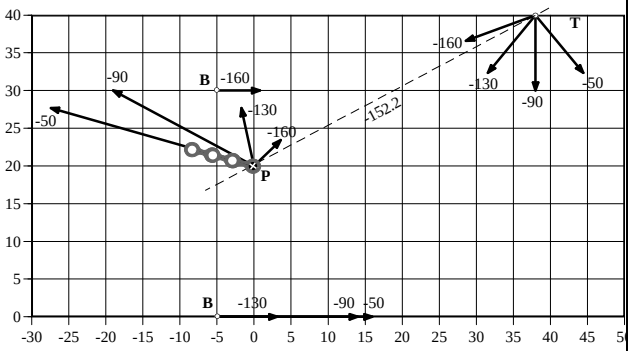

Fig. 5b. *c* = 20 mm, *a* = 38 mm.

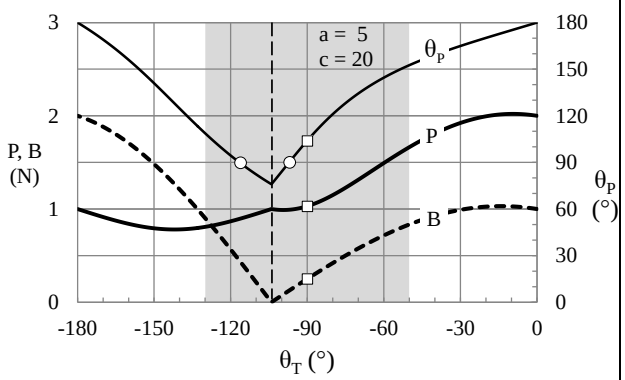

Fig. 6a

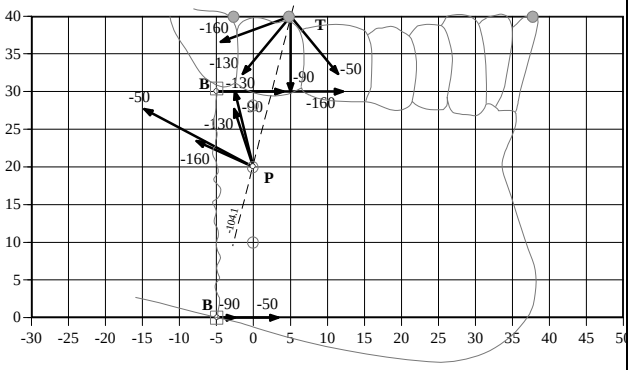

Fig. 6b. *c* = 20 mm, *a* = 5 mm.

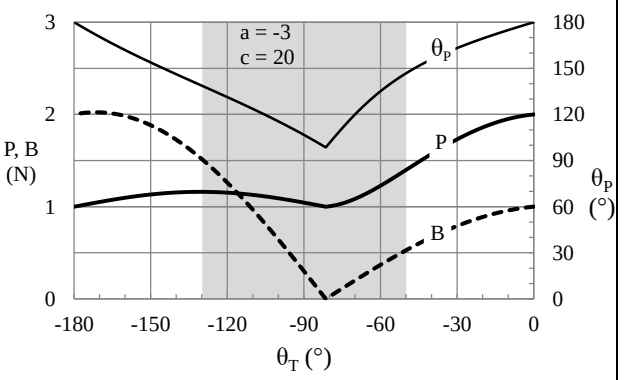

Fig. 7a

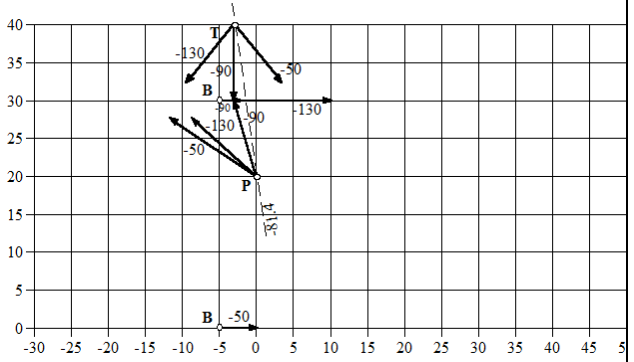

Fig. 7b. *c* = 20 mm, *a* = -3 mm.

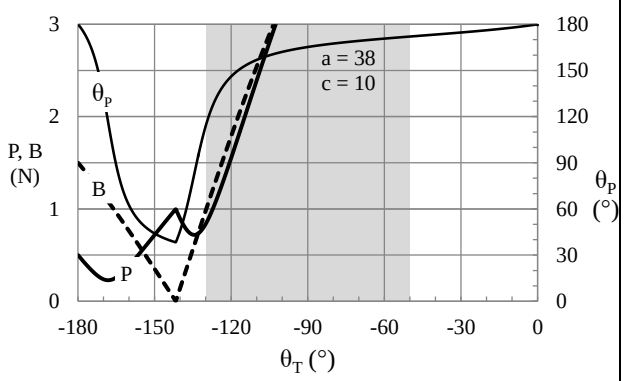

Fig. 8a

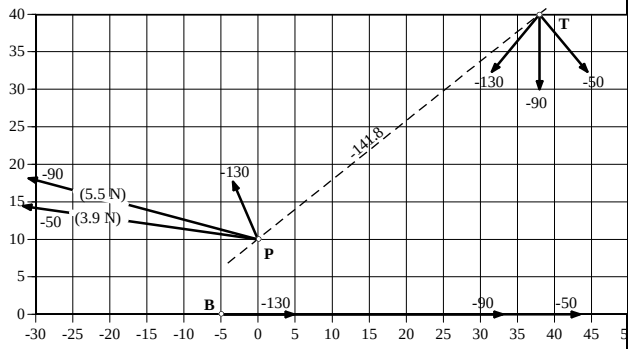

Fig. 8b. *c* = 10 mm, *a* = 38 mm.

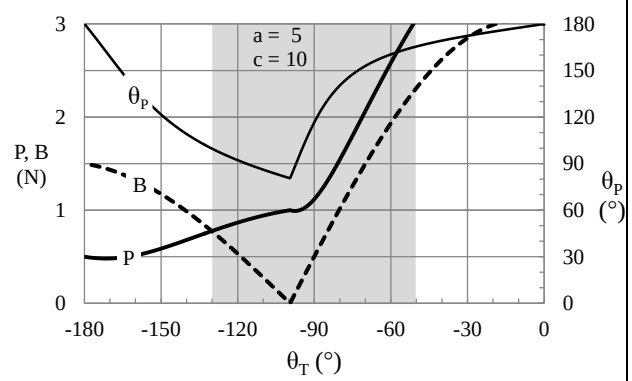

Fig. 9a

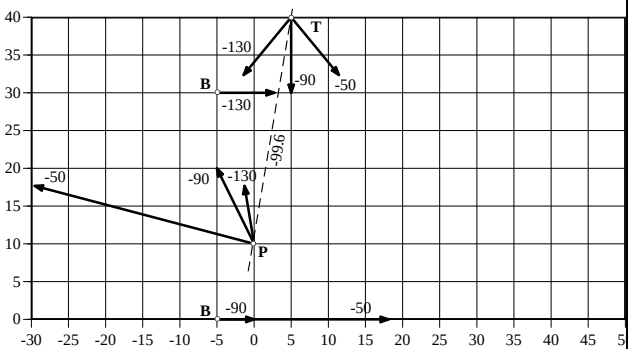

Fig. 9b. *c* = 10 mm, *a* = 5 mm.

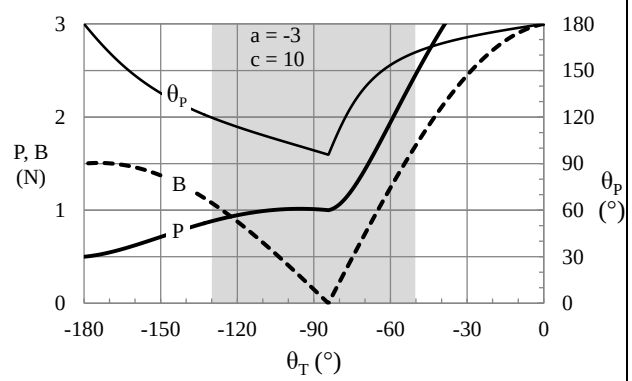

Fig. 10a

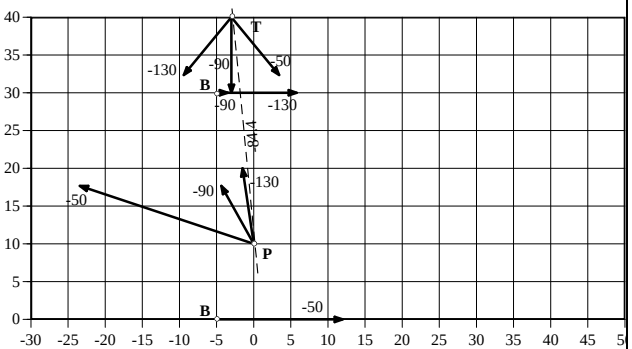

Fig. 10b. *c* = 10 mm, *a* = -3 mm.

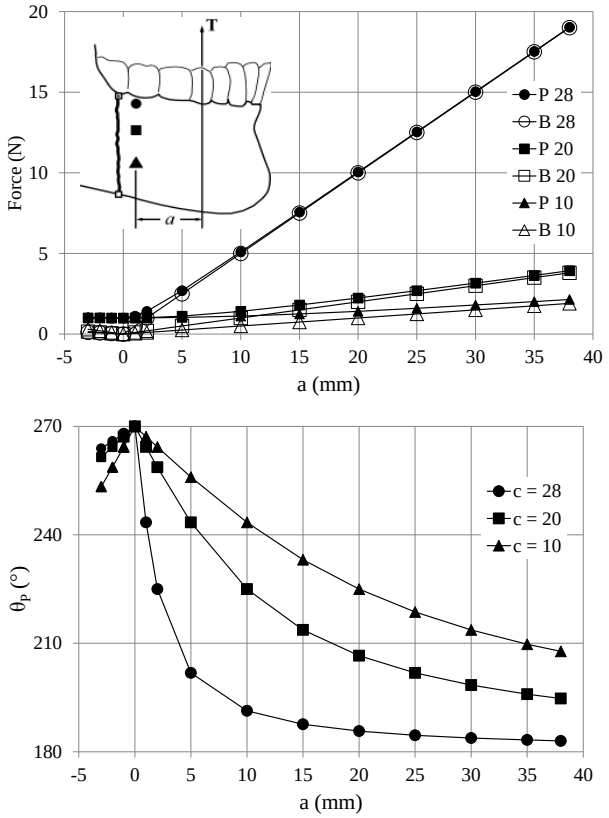

Figure 11. Results for sticky food (θ_T = +90°) with families of plate screw located at c = 28 (circles), 20 (squares) and 10 (triangles) mm. a ranges between -3 and 38 mm. The bone-bone contact force (**B**) is at the inferior or superior margin of the fracture if a < 0 mm or a > 0mm, respectively. The plate is always in tension.